THE ASTROPHYSICAL JOURNAL LETTERS, 899:L7 (4pp), 2020 August 10 https://doi.org/10.3847/2041-8213/aba89d

Constraining Cosmic-Ray Acceleration in the Magnetospheric Gaps of Sgr A*

Grigorios Katsoulakos[1], Frank M. Rieger[1,2], and Brian Reville[1]
[1] Max-Planck-Institut für Kernphysik, Saupfercheckweg 1, D-69117 Heidelberg, Germany; gkats@mpi-hd.mpg.de
[2] ZAH, Institut für Theoretische Astrophysik, Universität Heidelberg, Philosophenweg 12, D-69120 Heidelberg, Germany
Received 2020 June 26; revised 2020 July 17; accepted 2020 July 23; published 2020 August 6

Abstract

Sagittarius A* (Sgr A*) is a potential very high energy (VHE) γ-ray and cosmic-ray source. We examine limits to gap-type particle acceleration in the magnetosphere of Sgr A*, showing that in the current phase of activity proton acceleration to PeV energies is possible, with injection powers into the environment usually limited to several 10^{36} erg s^{-1}. Compton upscattering of ambient soft photons by gap-accelerated electrons could yield TeV emission compatible with the detected VHE point source. We explore the dependency of the results on changes in the accretion rate showing that higher stages in the past are unlikely to increase the power output unless the inner accretion flows itself changed its configuration.

Unified Astronomy Thesaurus concepts: High energy astrophysics (739); Black hole physics (159); Galactic cosmic rays (567); Galactic center (565)

1. Introduction

The center of the Milky Way harbors a supermassive black hole (BH) of mass $M_{\rm BH} \simeq 4.3 \pm 0.3 \times 10^6 M_\odot$ (e.g., Boehle et al. 2016; Gillessen et al. 2017). Its location is coincident with the compact radio source Sgr A* at a distance of $d \simeq 8.2$ kpc (Gravity Collaboration et al. 2019) that is known to exhibit periods of steady and variable nonthermal emission across the electromagnetic spectrum (e.g., see Genzel et al. 2010 for review).

At very high energies (VHEs) H.E.S.S. observations of the Galactic Center (GC) region have revealed a bright, pointlike γ-ray source spatially coincident with Sgr A*, along with extended (>100 pc) diffuse VHE emission correlated with massive gas-rich complexes in the Central Molecular Zone (CMZ; Aharonian et al. 2006; H.E.S.S. Collaboration et al. 2016, 2018). The latter correlation points to a hadronic origin of the diffuse emission where the γ-rays are produced in interactions of PeV protons with ambient gas. The spatial map of the diffuse VHE emission can thus be used to estimate the radial distribution of cosmic-ray (CR) protons within the CMZ. The resultant CR distribution appears compatible with quasi-continuous injection of >100 TeV protons from the vicinity of Sgr A*, and diffusive propagation for $\sim 10^4$ yr (H.E.S.S. Collaboration et al. 2016, 2018). The γ-ray point source at the GC, on the other hand, shows a power-law-type VHE spectrum (photon index $\simeq 2.1 \pm 0.1$) from $\sim$(0.1–10) TeV along with evidence for a cutoff (see Aharonian et al. 2009; MAGIC Collaboration et al. 2020), probably related to absorption of VHE gamma-rays by the ambient radiation field, and exhibits a modest luminosity of $L_{\rm VHE} \sim 10^{35}$ erg s^{-1}.

The current quiescent bolometric luminosity of Sgr A* is rather low, at a level of $L_B \sim 10^{36}$ erg s^{-1} $\sim 2 \times 10^{-9}$ $L_{\rm Edd}$, suggesting that Sgr A* is accreting in a radiatively inefficient mode (e.g., Yuan & Narayan 2014). There is X-ray morphological evidence, however, that Sgr A* could have been brighter (i.e., temporarily exceeding 10^{38-39} erg s^{-1}) in the more recent past (e.g., Ponti et al. 2013; Zhang et al. 2015; Terrier et al. 2018). We note that in the more distant past (i.e., a few Myr ago) much higher accretion rates, up to several percent of the Eddington value, must have occurred if the Fermi bubbles are indeed caused by some former AGN-type jet activity (e.g., Guo & Mathews 2012; Yang et al. 2012).

Particle acceleration in the vicinity of the GC BH has been proposed as possible source for the observed VHE radiation and presumed CR injection (e.g., Aharonian & Neronov 2005a, 2005b; Levinson & Rieger 2011; H.E.S.S. Collaboration et al. 2016). In this Letter we revisit the potential of magnetospheric, gap-type particle acceleration for facilitating VHE and CR production. This is done by drawing on an advanced steady gap model (Katsoulakos & Rieger 2020) that allows us to incorporate realistic ambient radiation fields.

2. The Galactic Center BH and Vicinity

We assume that the BH in Sgr A* (horizon scale $r_g = G M_{\rm BH}/c^2$) is rotating with angular momentum close to its maximum $\lesssim G M_{\rm BH}^2/c$. The magnetosphere is threaded by a magnetic field whose strength is approximately comparable to the equipartition value $B_H \simeq 10^6\, \dot{m}^{1/2}$ G, where $\dot{m} = \dot{M}/\dot{M}_{\rm Edd}$ denotes the source accretion rate in terms of the Eddington one, $\dot{M}_{\rm Edd} \simeq 0.1 M_\odot$ yr^{-1}. Radio (millimeter) polarization measurements indicate that the current accretion rate close to the BH is of order $\dot{M} \sim 10^{-8} M_\odot$ yr^{-1} (Bower et al. 2018), while radiative GRMHD models tend to favor even lower values, e.g., $\dot{M} \sim 10^{-9} M_\odot$ yr^{-1} (Drappeau et al. 2013). As noted above, a higher accretion activity might have been occurring in the past given the rich gas reservoir present in the GC vicinity (see Genzel et al. 2010). The above values suggest a typical field strength of $B_H \sim 100$ G for the present time, roughly compatible with other estimates (Dexter et al. 2010; Eatough et al. 2013).

In general, the soft photon field from the innermost parts of the accretion flow provide a major ingredient for the formation of pair cascades in the charge-starved regions (i.e., gaps) of BH magnetospheres (Levinson & Rieger 2011; Hirotani et al. 2017; Katsoulakos & Rieger 2020). In the following, we assume the inner accretion flow in Sgr A* to be hot and radiatively inefficient (ADAF), though possibly being supplemented by a cool gas phase on larger scales (e.g., Yuan & Narayan 2014; Murchikova et al. 2019). We use a simplified ADAF description (Mahadevan 1997) to characterize the ambient soft

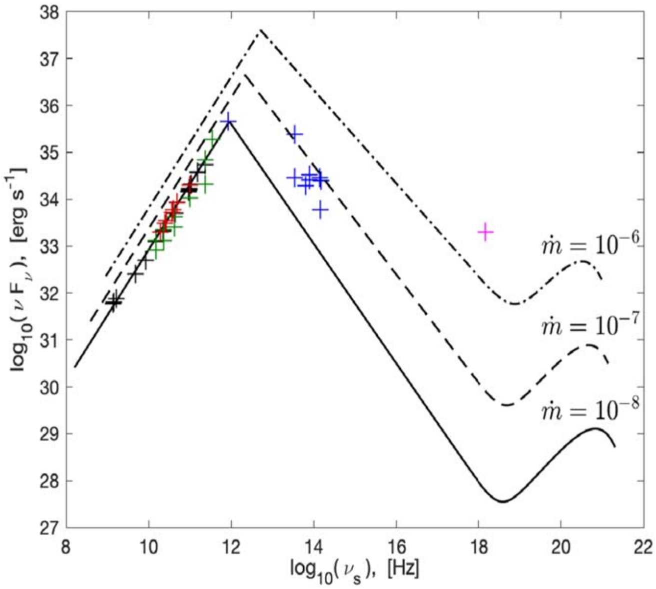

Figure 1. Reference ADAF spectra for accretion rates $\dot{m} = 10^{-8}$ (solid line), 10^{-7} (dashed), and 10^{-6} (dashed–dotted), respectively. A BH mass $M_{\rm BH} = 4.3 \times 10^6 M_\odot$ has been employed. Data are from Serabyn et al. (1997), Falcke et al. (1998), Baganoff et al. (2001), Hornstein et al. (2002), Zhao et al. (2003), Ghez et al. (2004), Schödel et al. (2011), and Brinkerink et al. (2015).

photon field and its possible variation with accretion rate. Figure 1 shows corresponding disk spectra for three different accretion rates, namely, for the current level, $\dot{m} = 10^{-8}$ (solid line), as well as for possible enhanced (past) accretion periods, i.e., $\dot{m} = 10^{-7}$ (dashed line), and, $\dot{m} = 10^{-6}$ (dashed–dotted line). To account for the experimental data using the current accretion rate (solid line in Figure 1), we further assume that 10% of the viscous turbulent energy is attributed to the electrons of the disk, and that the peak of the ADAF emission originates from the inner radius of the accretion disk located at $r \sim r_s$. The low-energy data are then satisfactorily described, while substantial deviations can become apparent toward higher energies. Since magnetospheric cascades and gap formation are primarily regulated by the low-energy part of the spectrum, i.e., the soft photons around the peak (Katsoulakos & Rieger 2020), such deviations are not expected to be critical for the present purpose. Note that our reference spectra should be considered as a convenient tool only, chosen such as to satisfy observational constraints. For detailed ADAF modeling of Sgr A*, we refer to Yuan et al. (2003).

In principle, pair production in a hot accretion flow ($\gamma\gamma \to e^+e^-$) can lead to charge injection into the BH magnetosphere. The charge density produced by annihilating MeV photons is of the order $n_\pm/n_{\rm GJ} \sim 4 \times 10^{11} \dot{m}^{7/2}$ (Levinson & Rieger 2011). Hence, for $\dot{m} \lesssim 10^{-4}$ the charge density falls short of the Goldreich–Julian (GJ) density $n_{\rm GJ}$, resulting in regions of incomplete electric field screening ($\boldsymbol{E} \cdot \boldsymbol{B} \neq 0$), the so-called "gaps." Under these conditions, pair cascades triggered within these regions can load the magnetosphere with a significant amount of charges.

3. Steady Gap Acceleration

The parallel electric field component $\mathcal{E}_{||}$ facilitating particle acceleration obeys the generalized Gauss's law (e.g., Katsoulakos & Rieger 2020)

$$\nabla \cdot \left(\frac{\mathcal{E}_{||}}{\alpha_l}\right) = 4\pi(\rho_e - \rho_{\rm GJ}), \quad (1)$$

where ρ_e is the actual charge density, $\rho_{\rm GJ}$ is the GJ charge density, and α_l is the Lapse function (Thorne & MacDonald 1982). The electric field is caused by the difference of the actual charge density relative to the GJ value.

Seed electron–positron pairs injected into the gap region (of size h) will be accelerated along $\mathcal{E}_{||}$, with their energies being limited by curvature and inverse Compton (IC) losses. The resultant γ-rays will undergo $\gamma\gamma$ annihilation with soft photons of the accretion disk, providing additional pairs to the gap. These secondary leptons will then also experience gap acceleration and γ-ray emission, triggering a third generation of leptons, and so on. The ensuing pair cascade develops until the charge density becomes sufficiently large to screen the parallel electric field.

The full gap structure, i.e., the distributions of the parallel electric field, the particle energy, the charge, and the γ-ray photon densities, can be derived by numerical integration of Gauss's law along with the equations of motion and continuity for the pairs, and the Boltzmann equation for the γ-ray photons (e.g., Hirotani et al. 2017; Levinson & Segev 2017; Katsoulakos & Rieger 2020). In addition to the BH mass and accretion rate, the magnetospheric current is a central parameter for steady gap models. Defined as $J_0 = (\rho_e^- - \rho_e^+)c\sqrt{1 - 1/\Gamma_e^2}$, where $\rho_e^\pm$ represents the positron/electron charge density and Γ_e the lepton Lorentz factor, the current is a constant quantity along magnetic field lines. Since there is currently no strong evidence for jet activity in Sgr A* (though see also Issaoun et al. 2019), we explore gap solutions for low current values. We note that the steady-state solutions for $J_0 \gtrsim 0.25\,\rho_c c$ in our model do not maintain physically consistent values in all quantities throughout the gap, and we thus disregard them. Here $\rho_c = \Omega B_H / 2\pi c$ is the effective GJ charge density. In the subsections below, we present gap solutions for different accretion regimes following the approach presented in Katsoulakos & Rieger (2020).

3.1. Results for the Current Accretion Stage

Figure 2(a) summarizes the electric field solutions for the present accretion rate ($\dot{m} = 10^{-8}$) adopting six different values for the magnetospheric current, ranging from $J_o^* = -0.01$ to $J_o^* = -0.244$, where $J_o^* = J_o/(c\,\rho_c)$. A field line inclination $\theta = 30°$, a soft photon source size $r_d = 5\,r_g$, and a BH mass $M_{\rm BH} = 4.3 \times 10^6 M_\odot$ have been adopted throughout.

As can be seen, the gap extension increases as the global current increases. Roughly speaking, we obtain gap sizes of the order of r_g for the chosen parameters; see Table 1. Small current values (e.g., $J_o^* = -0.01$) lead to highly underdense gaps, needing additional charge injection at the boundaries, while for higher current values (i.e., $J_o^* = -0.244$) the GJ charge density at the outer boundary is approached (see Figure 2(b)), so that force-free jet formation might occur, potentially contributing to the observed emission (e.g., Davelaar et al. 2018).

We determine the available voltage drop, $\Delta V_{\rm gap}$, by integrating $\mathcal{E}_{||}$ along the width of the gap, while the gap power $L_{\rm gap} \propto J_0\,\Delta V_{\rm gap}$ is determined by the rate of the lepton energy gain multiplied by the number of the particles within the gap. For the parameters used here, the gap luminosity typically

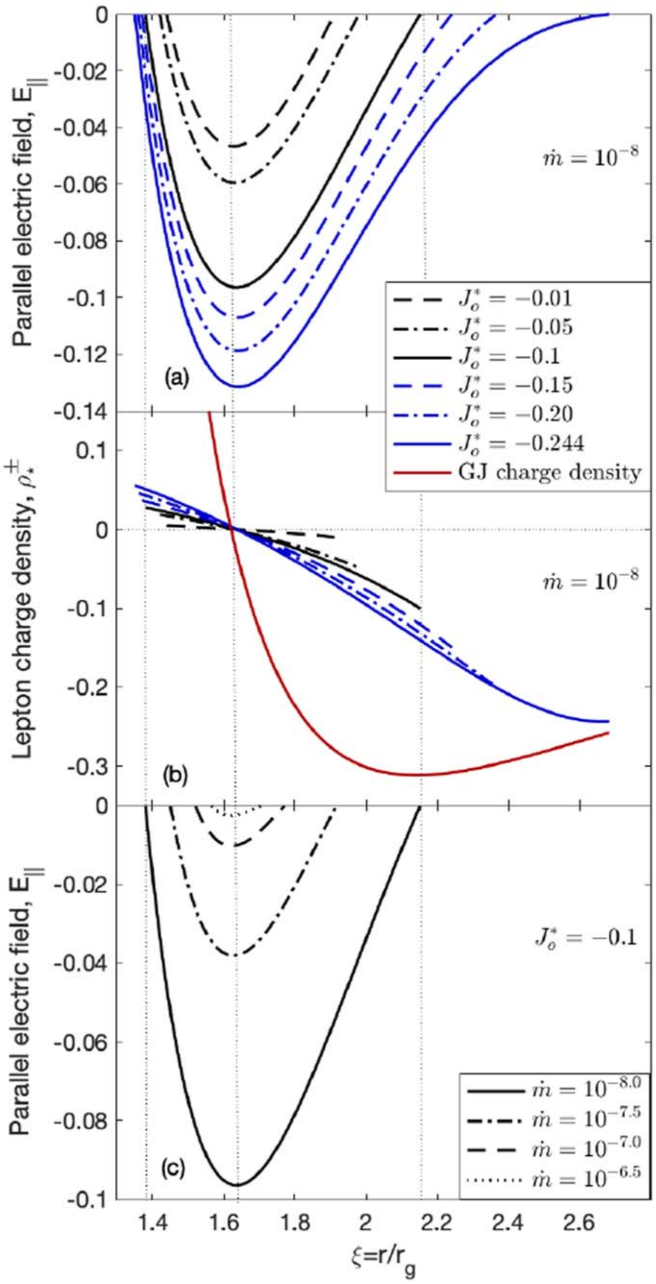

Figure 2. Distribution of the (normalized) parallel electric field component $\mathcal{E}_{\|}^{*r} = \mathcal{E}_{\|}^{r}/4\pi\ r_g\ \rho_c$, with fixed accretion rate $\dot{m} = 10^{-8}$, for different current values (upper panel). Normalized total charge density, $\rho_*^{\pm} = \rho_{\pm}/\rho_c$, also for fixed $\dot{m} = 10^{-8}$. Goldreich–Julian density in red for comparison (middle panel). Distribution of the (normalized) parallel electric field component $\mathcal{E}_{\|}^{*r}$ with fixed current $J_0^* = -0.1$, for different accretion rates (bottom panel).

constitutes only some fraction of the available accretion power $L_{\rm acc} = 5.4 \times 10^{37}$ erg s^{-1}.

In particular, Table 1 suggests that a power of $L_{\rm gap} \sim 10^{36}$ erg s^{-1} can be dissipated through the gap, e.g., via particle acceleration in a voltage difference of $\Delta V_{\rm gap} \sim 10^{15}$ V ($J_o^* = -0.1$) that could also facilitate PeV CR production. The inferred amount of power is comparable to the bolometric luminosity of the GC, indicating that gap-type particle acceleration and emission can potentially play a dominant role in Sgr A*. These results depend on the assumption that CRs within the gap essentially behave as test particles. The numbers presented above should thus be viewed as providing firm upper

Table 1
Gap Properties for the Current Accretion Stage

Global Current ($J_o^* = J_o/c\ \rho_c$)	Gap Size (h/r_g)	Voltage Drop ($\times 10^{15}$ V)	Gap Power ($\times 10^{35}$ erg s^{-1})
−0.01	0.47	0.40	0.35
−0.05	0.56	0.60	2.38
−0.10	0.77	1.27	8.87
−0.15	0.87	1.52	15.25
−0.20	1.01	1.82	24.26
−0.244	1.33	2.19	39.22

Note. Results for a BH mass of $M_{\rm BH} = 4.3 \times 10^6\ M_\odot$ and a fixed accretion rate $\dot{m} = 10^{-8}$.

Table 2
Gap Properties for Different Accretion Rates

Accretion Rate ($\dot{m} = \dot{M}/\dot{M}_{\rm Edd}$)	Gap Size (h/r_g)	Voltage Drop ($\times 10^{15}$ V)	Gap power ($\times 10^{35}$ erg s^{-1})
$10^{-8.0}$	0.77	1.27	8.87
$10^{-7.5}$	0.47	0.57	7.08
$10^{-7.0}$	0.25	0.15	3.37
$10^{-6.5}$	0.14	0.036	1.31

Note. Results for a fixed global current $J_o^* = -0.1$.

limits on possible CR power outputs. While CR injection has often been treated phenomenologically (e.g., Levinson & Boldt 2002; Neronov et al. 2009), a detailed scenario for CR injection into the gap would in principle be needed to quantify the amount of gap power carried by CRs.

Our gap solutions yield radiation-limited lepton Lorentz factors $\Gamma_e \lesssim 2 \times 10^8$. The associated curvature emission peaks at energies $\epsilon_{\rm cur} = (3/4\pi)(h\ c/r_g)\Gamma_e^3 \lesssim 0.4$ GeV, while IC emission reaches up to $\epsilon_{ic} \sim \Gamma_e m_e c^2 \sim 10^2$ TeV. Absorption of multi-TeV γ-rays in the ADAF photon fields decisively contributes to the cascade development in the gap. The observed γ-ray spectrum of Sgr A* in fact shows a cutoff above $\epsilon_c \sim 10$ TeV. Since photons with ϵ_c preferentially interact with soft photons of $\epsilon_s \sim 0.1$ eV, having a spectral luminosity $L_s \sim 10^{34}$ erg s^{-1} (Figure 1), the characteristic optical depth $\tau_{\gamma\gamma} = \sigma_{\gamma\gamma}\ n_s\ r_g$ is of order $\tau_{\gamma\gamma} \sim 0.03$, using $\sigma_{\gamma\gamma} \approx 0.2\ \sigma_\tau$ and $n_s = L_s/4\pi\ r_g^2\ c\ \epsilon_s$. This suggests that VHE photons of energy $\epsilon \leqslant \epsilon_c$ are able to escape from the BH vicinity, consistent with observations. Hence, it is possible that at the current epoch magnetospheric processes in Sgr A* may drive both TeV γ-ray as well as PeV CR production.

3.2. Results for Past Accretion Stages

Changes in the accretion environment will impact the gap characteristics. To investigate structural variations of the gap due to possible changes in the accretion rate in the past, we also explore higher values, up to $\dot{m} = 10^{-6.5}$, while keeping the current constant ($J_o^* = -0.1$). The results are shown in Figure 2(c) and Table 2.

As the ambient soft photon field becomes stronger and cascade formation more efficient with higher accretion rates, the gap width essentially decreases with increasing accretion rate, i.e., down to $h \sim 0.1\ r_g$ for $\dot{m} = 10^{-6.5}$. As a consequence, the available voltage difference and gap power decrease (see Katsoulakos & Rieger 2018). Thus, despite the fact that the magnetic field strength threading the horizon increases, the voltage difference falls, $\Delta V_{\rm gap} \lesssim 10^{15}$ V for $\dot{m} \geqslant 10^{-7.5}$, diminishing the potential for PeV CR production. Similarly, achievable electron Lorentz factors are reduced to $\Gamma_e \sim 6 \times 10^6$ for $\dot{m} = 10^{-6.5}$. Table 2 suggests an approximate dependence $\Delta V_{\rm gap} \propto \dot{m}^{-1}$ and $L_{\rm gap} \propto \dot{m}^{-0.6}$ over the range considered.

4. Conclusions

The above results suggest that at the present accretion stage, the BH in Sgr A* is in theory a rather effective electron and CR accelerator. As such, IC upscattering in Sgr A* could in principle contribute to the GC point source seen by current VHE instruments (e.g., Aharonian et al. 2009; Archer et al. 2016; MAGIC Collaboration et al. 2020). While full radiative modeling is required, a spectral cutoff above ∼10 TeV, related absorption of VHE gamma-rays by the ambient disk photon field is likely to remain a persistent feature of gap-related VHE emission. With its superior resolution, the upcoming Cherenkov Telescope Array will soon make it possible to probe deeper into the true nature of the GC VHE source (Cherenkov Telescope Array Consortium et al. 2019). Complementary Event Horizon Telescope observations are likely to shed further light on the innermost accretion flow in Sgr A* (Event Horizon Telescope Collaboration et al. 2019).

The accessible voltage differences in the BH magnetosphere of Sgr A* can exceed $\sim 10^{15}$ V, allowing for PeV CR production. Our results suggest the power for quasi-continuous CR injection into the GC region to be limited to several 10^{36} erg s^{-1}. If the diffuse VHE emission in the CMZ were to be related to the GC BH (H.E.S.S. Collaboration et al. 2016), this would thus constrain the (average) spatial diffusion coefficient within the CMZ to $D \lesssim 10^{29}$ cm^2 s^{-1} for >10 TeV protons. While restrictive, this would still be compatible with empirical diffusion models suggesting $D \simeq 5 \times 10^{28}$ $(E/10\,{\rm TeV})^{1/3}$ cm^2 s^{-1} (e.g., Strong et al. 2007; Fujita et al. 2017). Progress in characterizing the turbulence field structures that ultimately determine the CR transport properties within the CMZ will help to better assess this. In principle, magnetospheric gaps are likely to produce rather hard and narrow particle distributions. While propagation effects and variable accretion rate will modify any source spectra when viewed on larger spatial scales, a signature of CR acceleration from the gaps might reveal itself through a harder spectral component, observable closer in.

Though the GC BH could be a CR PeVatron, no significant contribution to the observed Galactic CR spectrum is expected under normal conditions. In fact, provided the disk remains ADAF type, the gap power and potential do not increase considering higher accretion stages in the past, as the gap extension becomes smaller with higher accretion rates. An exception to this could be possible, however, for extreme states in the past in which the inner accretion flow changed its configuration. This might have occurred during the GC phase associated with the generation of the Fermi bubbles ∼1–10 Myr ago (e.g., Guo & Mathews 2012; Fujita et al. 2017; Jaupart et al. 2018), and deserves further investigation.

While the results shown here are based on a simplified disk and magnetic field model, we expect them to be quite generic for quasi-steady gap models. Exploring varying disk emission and the characteristics of non-steady gaps where the lepton multiplicity could potentially exceed one (e.g., Levinson & Cerutti 2018) is a goal of future work.

We are grateful to Felix Aharonian, John Kirk, and Heino Falcke for comments and discussions. F.M.R. acknowledges funding by a DFG Heisenberg Fellowship under RI 1187/6-1.

ORCID iDs

Grigorios Katsoulakos https://orcid.org/0000-0002-8155-5969
Frank M. Rieger https://orcid.org/0000-0003-1334-2993
Brian Reville https://orcid.org/0000-0002-3778-1432

References

Aharonian, F., Akhperjanian, A. G., Anton, G., et al. 2009, A&A, 503, 817
Aharonian, F., Akhperjanian, A. G., Bazer-Bachi, A. R., et al. 2006, Natur, 439, 695
Aharonian, F., & Neronov, A. 2005a, ApJ, 619, 306
Aharonian, F., & Neronov, A. 2005b, Ap&SS, 300, 255
Archer, A., Benbow, W., Bird, R., et al. 2016, ApJ, 821, 129
Baganoff, F. K., Bautz, M. W., Brandt, W. N., et al. 2001, Natur, 413, 45
Boehle, A., Ghez, A. M., Schödel, R., et al. 2016, ApJ, 830, 17
Bower, G. C., Broderick, A., Dexter, J., et al. 2018, ApJ, 868, 101
Brinkerink, C. D., Falcke, H., Law, C. J., et al. 2015, A&A, 576, A41
Cherenkov Telescope Array Consortium, Acharya, B. S., Agudo, I., et al. 2019, Science with the Cherenkov Telescope Array (Singapore: World Scientific)
Davelaar, J., Mościbrodzka, M., Bronzwaer, T., & Falcke, H. 2018, A&A, 612, A34
Dexter, J., Agol, E., Fragile, P. C., & McKinney, J. C. 2010, ApJ, 717, 1092
Drappeau, S., Dibi, S., Dexter, J., Markoff, S., & Fragile, P. C. 2013, MNRAS, 431, 2872
Eatough, R. P., Falcke, H., Karuppusamy, R., et al. 2013, Natur, 501, 391
Event Horizon Telescope Collaboration, Akiyama, K., Alberdi, A., et al. 2019, ApJL, 875, L2
Falcke, H., Goss, W. M., Matsuo, H., et al. 1998, ApJ, 499, 731
Fujita, Y., Murase, K., & Kimura, S. S. 2017, JCAP, 04, 037
Genzel, R., Eisenhauer, F., & Gillessen, S. 2010, RvMP, 82, 3121
Ghez, A. M., Wright, S. A., Matthews, K., et al. 2004, ApJL, 601, L159
Gillessen, S., Plewa, P. M., Eisenhauer, F., et al. 2017, ApJ, 837, 30
Gravity Collaboration, Abuter, R., Amorim, A., et al. 2019, A&A, 625, L10
Guo, F., & Mathews, W. G. 2012, ApJ, 756, 181
H.E.S.S. Collaboration, Abdalla, H., Abramowski, A., et al. 2018, A&A, 612, A9
H.E.S.S. Collaboration, Abramowski, A., Aharonian, F., et al. 2016, Natur, 531, 476
Hirotani, K., Pu, H.-Y., Lin, L. C.-C., et al. 2017, ApJ, 845, 77
Hornstein, S. D., Ghez, A. M., Tanner, A., et al. 2002, ApJL, 577, L9
Issaoun, S., Johnson, M. D., Blackburn, L., et al. 2019, ApJ, 871, 30
Jaupart, É., Parizot, É., & Allard, D. 2018, A&A, 619, A12
Katsoulakos, G., & Rieger, F. M. 2018, ApJ, 852, 112
Katsoulakos, G., & Rieger, F. M. 2020, ApJ, 895, 99
Levinson, A., & Boldt, E. 2002, APh, 16, 265
Levinson, A., & Cerutti, B. 2018, A&A, 616, A184
Levinson, A., & Rieger, F. 2011, ApJ, 730, 123
Levinson, A., & Segev, N. 2017, PhRvD, 96, 123006
MAGIC Collaboration, Acciari, V. A., Ansoldi, S., et al. 2020, arXiv:2006.00623
Mahadevan, R. 1997, ApJ, 477, 585
Murchikova, E. M., Phinney, E. S., Pancoast, A., & Blandford, R. D. 2019, Natur, 570, 83
Neronov, A. Y., Semikoz, D. V., & Tkachev, I. I. 2009, NJPh, 11, 065015
Ponti, G., Morris, M. R., Terrier, R., & Goldwurm, A. 2013, in Cosmic Rays in Star-Forming Environments, ed. D. F. Torres & O. Reimer (Berlin: Springer), 331
Schödel, R., Morris, M. R., Muzic, K., et al. 2011, A&A, 532, A83
Serabyn, E., Carlstrom, J., Lay, O., et al. 1997, ApJL, 490, L77
Strong, A. W., Moskalenko, I. V., & Ptuskin, V. S. 2007, ARNPS, 57, 285
Terrier, R., Clavel, M., Soldi, S., et al. 2018, A&A, 612, A102
Thorne, K. S., & MacDonald, D. 1982, MNRAS, 198, 339
Yang, H. Y. K., Ruszkowski, M., Ricker, P. M., Zweibel, E., & Lee, D. 2012, ApJ, 761, 185
Yuan, F., & Narayan, R. 2014, ARA&A, 52, 529
Yuan, F., Quataert, E., & Narayan, R. 2003, ApJ, 598, 301
Zhang, S., Hailey, C. J., Mori, K., et al. 2015, ApJ, 815, 132
Zhao, J.-H., Young, K. H., Herrnstein, R. M., et al. 2003, ApJL, 586, L29